ISSN 1845–8319

FORBUSH DECREASES ASSOCIATED TO STEALTH CORONAL MASS EJECTIONS

B. HEBER[1], C. WALLMANN[1], D. GALSDORF[1], K. HERBST[1], P. KÜHL[1]
M. DUMBOVIC[2], B. VRŠNAK[2], A. VERONIG[3], M. TEMMER[3],
C. MÖSTL[3] and S. DALLA[4].

[1] *Institute for Experimental and Applied Physics, Christian-Albrechts-University Kiel, Germany*
[2] *Hvar Observatory, Faculty of Geodesy, University of Zagreb, Kačićeva 26, HR–10000 Zagreb, Croatia*
[3] *Institute of Physics/Kanzelhöhe Observatory, University of Graz, Austria*
[4] *Jeremiah Horrocks Institute, University of Central Lancashire, Preston, PR1 2HE, UK*

Abstract. Interplanetary coronal mass ejections (ICMEs) are structures in the solar wind that are the counterparts of coronal mass ejections (CMEs) at the Sun. It is commonly believed that enhanced magnetic fields in interplanetary shocks and solar ejecta as well as the increased turbulence in the solar wind sheath region are the cause of Forbush decreases (FDs) representing decreases of galactic cosmic ray (GCR) intensities. Recently, stealth CMEs i.e. CMEs with no apparent solar surface association have become a subject in recent studies of solar activity. Whether all of such stealth CMEs can drive a FD is difficult to investigate on the basis of neutron monitor NM measurements because these measurements not only reflect the GCR intensity variation in interplanetary space but also the variation of the geomagnetic field as well as the conditions in the Earth atmosphere. Single detector counter from spacecraft instrumentation, here SOHO and Chandra EPHIN, exceed counting statistic of NMs allowing to determine intensity variation of less than 1‰ in interplanetary space on the basis of 30 minute count rate averages. Here we present the ongoing analysis of eleven stealth CMEs.

Key words: Galactic Cosmic Rays - Forbush decreases - Stealth CMEs

1. Introduction

Forbush (1937) and Hess and Demmelmair (1937) were the first to observe short-term intensity decreases using ionization chambers, known as Forbush decreases (FDs). There are two different types of FDs, one associated with the passage of Corotating Interaction Regions (CIRs, see *e.g.* Richardson, 2004) and the other with interplanetary coronal mass ejections (ICMEs, see *e.g.* Cane, 2000; Richardson and Cane, 2011). Depending on how an observer crosses through the ICME structure, he will measure an intensity decrease that is caused by enhanced scattering in the sheath region and/or an intensity decrease due to the ICME itself (see Figure 1 from Richardson and Cane, 2011). The largest FDs typically involve ejecta with magnetic cloud (MC) properties (Richardson and Cane, 2011). The amplitude of these variations are still small. Several studies on FDs have been performed utilizing neutron monitors (e.g. Belov *et al.*, 2014, and references in there). These authors found amplitudes that can be as low as a few ‰. Statistically significant measurements need to provide detection of changes in the counting rate of less than 1‰ on time scales of several minutes. In addition, the effects should not be masked by other impact factors like geomagnetic activity (Papaioannou *et al.*, 2010). Therefore, Richardson *et al.* (1996) suggested to utilize single counter measurements. The Electron Proton Helium INstrumant (EPHIN, Müller-Mellin *et al.*, 1995), which will be used in this study, provides such single counting rates as discussed in detail by Kühl *et al.* (2015).

MCs are a subset of ICMEs that have a smooth rotation in an enhanced magnetic field, low proton temperatures and low plasma-β (*e.g.* Klein and Burlaga, 1982; Zurbuchen and Richardson, 2006; Riley and Richardson, 2013) and are found in about one third of the observed ICMEs (Richardson and Cane, 2010). There have been many efforts in modeling of FD (*e.g.* Le Roux and Potgieter, 1991; Cane *et al.*, 1995; Wibberenz *et al.*, 1997, 1998; Krittinatham and Ruffolo, 2009; Kubo and Shimazu, 2010). The studies have shown that the intensity decrease caused by enhanced diffusion in the sheath region of the CME and the propagation into magnetically closed structures are very different and therefore should be modeled separately (see also Cane, 2000).

Since it is difficult to resolve the relative contribution of these mechanism by measurements of FDs that are caused by ICMEs that drives on the one hand a turbulent sheath region and on the other hand contains MC structures one needs to focus on slow CMEs (MCs) that are carried by the ambient solar wind. From this point of view, good candidates are the so-called "stealth" CMEs which do not show any recognizable/distinct take-off signature neither in the low corona nor in the chromosphere (Robbrecht *et al.*, 2009; Wang *et al.*, 2011; Howard and Harrison, 2013). Such events are generally slow, with a more gradual formation and are probably launched

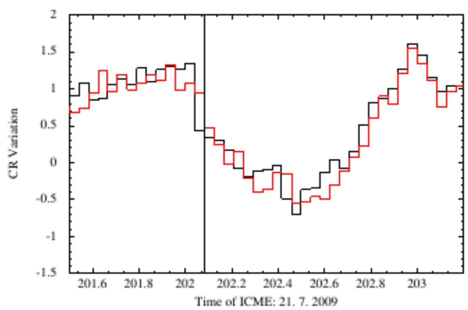

Figure 1: The figure displays hourly averaged variation of the count rate of detector F aboard SOHO (black curve) and Chandra (red curve) during the passage of a magnetic cloud. SOHO data have been shifted by the time the solar wind needs to move from SOHOs position to Chandra.

from larger heights than most of the CMEs (Ma *et al.*, 2010; D'Huys *et al.*, 2014; Kilpua *et al.*, 2014), leading to a much weaker energy release than under normal conditions (Schrijver *et al.*, 2011). In addition, they are often preceded by a nearby CME and/or are found in the vicinity of the polar coronal hole, *i.e.* originate in a region of weak downward force from the overlying magnetic field (D'Huys *et al.*, 2014). Therefore, the effect on lower layers is not strong enough to be observed in EUV range or in chromospheric spectral lines. Since most of such events travel with the solar wind, they are not likely to form a sheath region and are therefore suitable for FD ejecta-effect consideration.

2. Observations and Event Selection

The observations presented here were made by the Electron Proton Helium INstrument (EPHIN) aboard the SOHO and the Chandra spacecraft (Müller-Mellin *et al.*, 1995). While SOHO orbits the Lagrangian point L1 since 1996, Chandra, launched July 23, 1999, is on an elliptical orbit around the Earth. In contrast to SOHO, Chandra's orbit includes crossings of the radiation belts, magnetosphere as well as bow shock with an orbital period of 63.5 hours. The hourly averaged variation of the single detector F aboard SOHO (black curve) and Chandra (red curve) in % are shown during the crossing of a magnetic cloud in Fig. 1. SOHO data have been shifted by the time the solar wind needs to move from SOHOs position to Chandra. From the graph it is obvious that taking into account the measured solar wind speed and the distance between the two spacecraft the count rate variations agree very well with each other.

A list of 11 stealth CMEs was provided by Kilpua *et al.* (2014). In what follows we first analyze the time profile of the single detector count rates and search for time profiles that are symmetric, indicating a FD that is probably caused solely by a MC. Out of the 11 candidates 5 candidates show a symmetric structure with the count rate reaching the same level again after the passage of the MC. From these five ICMEs three drive a sheath region. One of the two remaining cases, the event from July 10, 2009, is displayed in Fig. 2. From top to bottom the magnetic field strength and fluctuations, field components, plasma density and thermal speed, solar wind speed and plasma-β, and finally, the variation of the single detector count rates from SOHO and Chandra EPHIN are shown. The MC start and end times are given by vertical solid lines.

Since stealth CMEs are usually slow, it is expected that they don't drive a frontal sheath. The example displayed in Fig. 2 shows a MC that moves at the speed which is almost adjusted to the solar wind speed and shows only a weak expansion (the speed decreases from 340 km/s at the MC front to a value of 310 km/s at its rear). Consequently, the region ahead of the MC does not show an obvious sheath structure. There are only some signatures that could be interpreted as a weak sheath phenomenon: from DOY 201.0 (vertical dashed line in Fig. 2) the magnetic field increases from 3 nT before the sheath-like structure to 6 nT at the MC front (DOY 202.1). At the same time, the velocity increases from 290 km/s to 340 km/s. The whole period is characterized by increased temperature and turbulence. This sheath-like structure could be attributed to a combined effect of the MC expansion and radial propagation. Interestingly, a small effect in CR count is also observed (decrease of 1.1 %).

The start of the MC is characterized by the temperature and drop in plasma-β, as well as the start of the smooth rotation of the magnetic field component B_z, as seen in Fig. 2. We also observe a change in the speed profile (reversing from an increasing to a decreasing trend). Typical MC signatures (low T_p, low N_p, low β, smooth rotation in B, declining profile of v_p indicating expansion) are seen up to DOY 202.8 (vertical black dotted line in Fig. 2), after which we observe a small increase in the density and plasma β, drop in B and stabilization of v_p at 310 km/s. This region is followed by typical CIR signatures of increased turbulence, density and magnetic field starting at DOY 203.0, followed by a sudden drop in density and increase in temperature at the stream interface (DOY 203.2, vertical solid gray line in Fig. 2) and increasing speed profile from the start of the CIR and across the

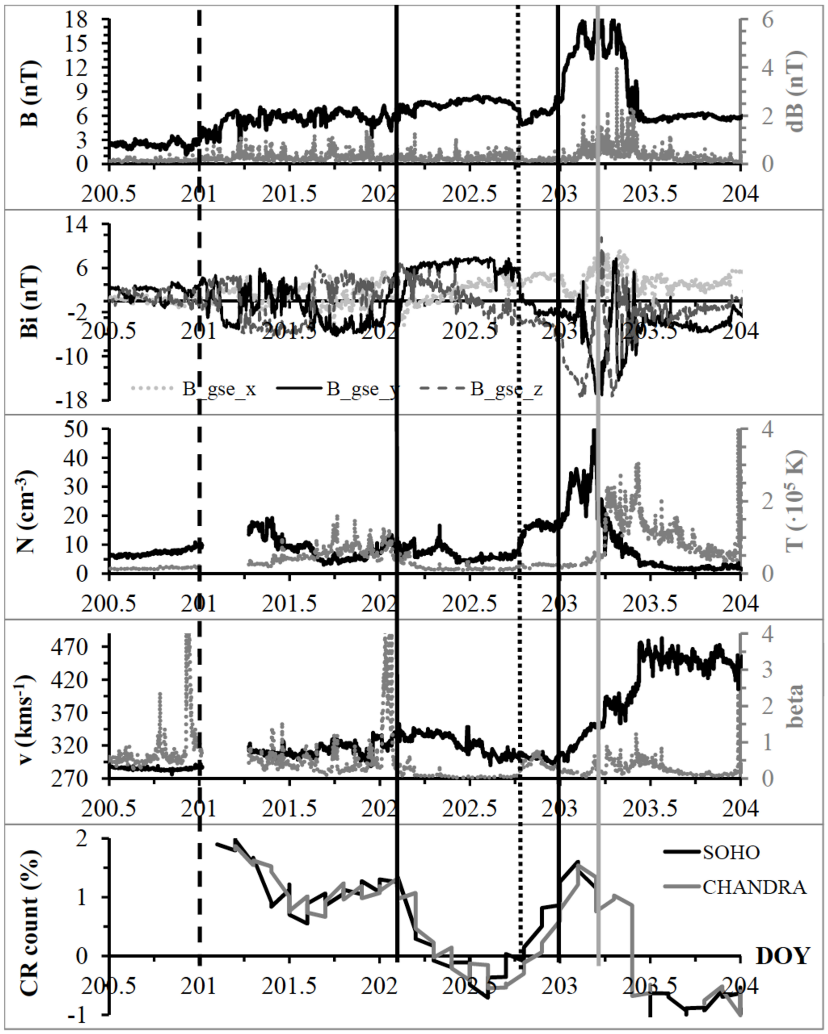

Figure 2: From top to bottom: Magnetic field strength and fluctuations (grey curve), components of the field, density and temperature (grey curve), solar wind speed and plasma beta parameter (grey curve) and variation of the single detector count rates from SOHO and Chandra EPHIN (grey curve) during the ICME crossings on July 10, 2009. Magnetic field data are taken from ACE satellite, whereas plasma data are taken or calculated based on WIND satellite data. Solid vertical lines represent start and end of MC. Dashed vertical line represents the start of the sheath-like region, whereas the dotted vertical line represents the end of typical MC-signature region. Gray vertical line marks stream interface.

stream interface. We assume that the region between DOY 202.8 and 203 belongs still to the MC, slightly "pushed" by the CIR behind, therefore as the end of MC we take DOY 203. Note that the discontinuity in magnetic field at DOY 202.8, which is caused by a change of the B_y component and is accompanied by a density increase that has the characteristic of a slow mode shock which is probably caused by the interaction of the MC and the heliospheric current sheath. Taking into account that the end of the MC could be anywhere between DOY 202.8, up to which we observe typical MC signatures, and DOY 202.2, where we observe a stream interface, it is reasonable to conclude that the end of MC is DOY 203 ± 0.2.

3. Summary and Conclusion

FDs that are caused by the passage of transient phenomena like shock waves driven by the interplanetary counterpart of the Coronal Mass Ejections (ICME) and the ICME itself, are caused by changing transport coefficients in the turbulent sheath region and/or in the MC. Most FD studies in the literature focus on ICMEs that drive a sheath region. Here we concentrate on a series of eleven stealth CME i.e. slow ICMEs that are characterized by a MC structure only. When using single detector count rates from EPHIN we found for all events a FD However, from the eleven events six events cause a classic FD time profile and only five the expected symmetric profile. From these events three ICMEs even drive a well developed sheath region. Thus two events remained from which we analyzed the event from July 10, 2009 in more detail.

The in-situ measurements for the corresponding event show typical MC signatures, with relatively weak magnetic field strength (B<10 nT) and typical duration of the order of 1 day. These observations are reflected by the FD, which shows typical ejecta-only properties. The observed FD corresponds to the duration of the MC, is symmetric and has a small amplitude (<several %). Therefore, this event represents a good test event for the modeling of ejecta only caused Forbush decreases.

Acknowledgements

This work has been supported in part by Croatian Science Foundation under the project 6212 ”Solar and Stellar Variability” and by MZOŚ/DAAD bilateral project CORAMOD. M.T. acknowledges funding by the Austrian Science Fund FWF: V195-N16. Chandra and SOHO/EPHIN are supported under Grant 50 OC 1302 by the German Bundesministerium für Wirtschaft through the Deutsches Zentrum für Luft- und Raumfahrt (DLR).

References

Belov, A., Abunin, A., Abunina, M., Eroshenko, E., Oleneva, V., Yanke, V., Papaioannou, A., Mavromichalaki, H., Gopalswamy, N., and Yashiro, S.: 2014, *Solar Physics* **289**(1), 3949.

Cane, H. V.: 2000, *Space Science Reviews* **93**(1), 55.

Cane, H. V., Richardson, I. G., and Wibberenz, G.: 1995, *International Cosmic Ray Conference* **4**, 377.

D'Huys, E., Seaton, D. B., Poedts, S., and Berghmans, D.: 2014, *The Astrophysical Journal* **795**(1), 49.

Forbush, S. E.: 1937, *Physical Review* **51**(1), 1108.

Hess, V. F. and Demmelmair, A.: 1937, *Nature* **140**(3), 316.

Howard, T. A. and Harrison, R. A.: 2013, *Solar Physics* **285**(1), 269.

Kilpua, E. K. J., Mierla, M., Zhukov, A. N., Rodriguez, L., Vourlidas, A., and Wood, B.: 2014, *Solar Phys.* **289**, 3773.

Klein, L. W. and Burlaga, L. F.: 1982, *Journal of Geophysical Research* **87**, 613.

Krittinatham, W. and Ruffolo, D.: 2009, *Astrophys. J.* **704**, 831.

Kubo, Y. and Shimazu, H.: 2010, *Astrophys. J.* **720**, 853.

Kühl, P., Banjac, S., Heber, B., Labrenz, J., Müller-Mellin, R., and Terasa, C.: 2015, *Central European Astrophysical Bulletin*, this issue.

Le Roux, J. A. and Potgieter, M. S.: 1991, *Astron. Astrophys.* **243**, 531.

Ma, S., Attrill, G. D. R., Golub, L., and Lin, J.: 2010, *The Astrophysical Journal* **722**(1), 289.

Müller-Mellin, R., Kunow, H., Fleißner, V., Pehlke, E., Rode, E., Röschmann, N., Scharmberg, C., Sierks, H., Rusznyak, P., McKenna-Lawlor, S., Elendt, I., Sequeiros, J., Meziat, D., Sanchez, S., Medina, J., Del Peral, L., Witte, M., Marsden, R., and Henrion, J.: 1995, *Solar Physics* **162**(1), 483.

Papaioannou, A., Malandraki, O., Belov, A., Skoug, R., Mavromichalaki, H., Eroshenko, E., Abunin, A., and Lepri, S.: 2010, *Solar Physics* **266**(1), 181.

Richardson, I. G.: 2004, *Space Science Reviews* **111**(3), 267.

Richardson, I. G. and Cane, H. V.: 2010, *Solar Physics* **264**(1), 189.

Richardson, I. G. and Cane, H. V.: 2011, *Solar Physics* **270**(2), 609.

Richardson, I. G., Wibberenz, G., and Cane, H. V.: 1996, *Journal of Geophysical Research* **101**(A), 13483.

Riley, P. and Richardson, I. G.: 2013, *Solar Phys.* **284**, 217.

Robbrecht, E., Patsourakos, S., and Vourlidas, A.: 2009, *arXiv.org* (1), 283.

Schrijver, C. J., Aulanier, G., Title, A. M., Pariat, E., and Delannée, C.: 2011, *Astrophys. J.* **738**, 167.

Wang, Y., Chen, C., Gui, B., Shen, C., Ye, P., and Wang, S.: 2011, *arXiv.org* (A), 4104.

Wibberenz, G., Cane, H. V., and Richardson, I. G.: 1997, *International Cosmic Ray Conference* **1**, 397.

Wibberenz, G., Le Roux, J. A., Potgieter, M. S., and Bieber, J. W.: 1998, *Space Sci. Rev.* **83**, 309.

Zurbuchen, T. H. and Richardson, I. G.: 2006, *Space Sci. Rev.* **123**, 31.